

Adenylation Enzyme Characterization Using γ - $^{18}\text{O}_4$ -ATP Pyrophosphate Exchange

Vanessa V. Phelan,¹ Yu Du,¹ John A. McLean,¹ and Brian O. Bachmann^{1,*}¹Department of Chemistry, Vanderbilt University, Nashville, TN 37204, USA*Correspondence: brian.bachmann@vanderbilt.edu

DOI 10.1016/j.chembiol.2009.04.007

SUMMARY

We present here a rapid, highly sensitive nonradioactive assay for adenylation enzyme selectivity determination and characterization. This method measures the isotopic back exchange of unlabeled pyrophosphate into γ - $^{18}\text{O}_4$ -labeled ATP via matrix-assisted laser desorption/ionization time-of-flight mass spectrometry (MS), electrospray ionization liquid chromatography MS, or electrospray ionization liquid chromatography-tandem MS and is demonstrated for both nonribosomal (TycA, ValA) and ribosomal synthetases (TrpRS, LysRS) of known specificity. This low-volume (6 μl) method detects as little as 0.01% (600 fmol) exchange, comparable in sensitivity to previously reported radioactive assays and readily adaptable to kinetics measurements and high throughput analysis of a wide spectrum of synthetases. Finally, a previously uncharacterized A-T didomain from anthramycin biosynthesis in the thermophile *S. reuinius* was demonstrated to selectively activate 4-methyl-3-hydroxyanthranilic acid at 47°C, providing biochemical evidence for a new aromatic β -amino acid activating adenylation domain and the first functional analysis of the anthramycin biosynthetic gene cluster.

INTRODUCTION

Synthetases play a key role in a range of cellular processes, particularly in those involving protein and peptide amide bond synthesis. In the case of ribosomal peptide synthesis, dedicated tRNA synthetases activate amino acids via adenylation, after which they are transferred by esterification to the 3' or 2' hydroxyl of cognate tRNA templates. In secondary metabolism, most peptide bonds are formed by nonribosomal peptide synthetases (NRPS). NRPS are multidomain systems that also transiently activate amino acids, including nonproteinogenic amino acids, via adenylation. This activation is catalyzed by adenylation (A) domains that subsequently interact with adjacent thiolation (T) domains (Figure 1A), in which pendant phosphopantetheinyl moieties covalently capture amino acid adenylates as thioesters prior to condensation (C) domain catalyzed reactions. NRPS are responsible for the biosynthesis of the peptide scaffolds of a large number of clinically significant natural product pharma-

ceuticals including penicillin, vancomycin, and rapamycin, to name a few (Fischbach and Walsh, 2006; Sieber and Marahiel, 2005).

The biochemical assay of decoupled synthetases poses practical challenges because most adenylation reactions are not formally catalytic. Isolated synthetases perform half-reactions (Figure 1B) for subsequent amino acid (thio)esterification that are nearly stoichiometric with regard to their respective tRNA/T domains and aminoacyl adenylates are tightly bound enzyme intermediates. Conventionally, adenylation enzyme selectivity has been assayed using the ATP- ^{32}PPI (pyrophosphate) isotope exchange assay. In this method, the synthetase is incubated with excess ^{32}PPI , amino acid, and ATP, and the reversible back exchange of labeled ^{32}PPI into ATP is monitored by solid-phase capture of ATP on activated charcoal followed by scintillation counting. This method, in use for more than half a century (Lee and Lipmann, 1975; Linne and Marahiel, 2004a), is highly sensitive and modern variants have recently been developed for high-throughput and kinetics applications (Otten et al., 2007). The primary drawbacks of the assay are that it requires relatively large amounts of radioactive PPI (0.2 μCi /experiment) and extensive liquid handling of highly radioactive materials. Moreover, the solid-phase capture step is an indirect measure of exchange and high background signal can complicate data analysis.

This study describes a nonradioactive mass spectrometry (MS)-based PPI exchange assay. To validate the method, we first assayed previously characterized synthetases: TycA, responsible for L-phenylalanine activation during tyrocidine biosynthesis (Pfeifer et al., 1995); ValA, an "orphan" A domain responsible for valine activation (Du and Shen, 1999); and *E. coli* tRNA synthetases TrpRS and LysRS (Joseph and Muench, 1971; Stern et al., 1966). Subsequently, we assayed the specificity of ORF21, a recently described uncharacterized A-T didomain of the anthramycin gene cluster (Hu et al., 2007), providing the first biochemical evidence for the anthramycin biosynthetic pathway.

RESULTS

Mass sensitive observation of PPI exchange can hypothetically detect adenylation domain catalyzed mass shifts on either side of the exchange equation. As back exchange is favored by using PPI in excess, we introduced a heavy atom label in the starting material as γ - $^{18}\text{O}_4$ -ATP. γ - $^{18}\text{O}_4$ -ATP is commercially available or alternatively can be synthesized chemically (Hoard and Ott, 1965). Conditions for MS isotope exchange were based on previously reported assay methods (Linne and Marahiel, 2004a; Otten

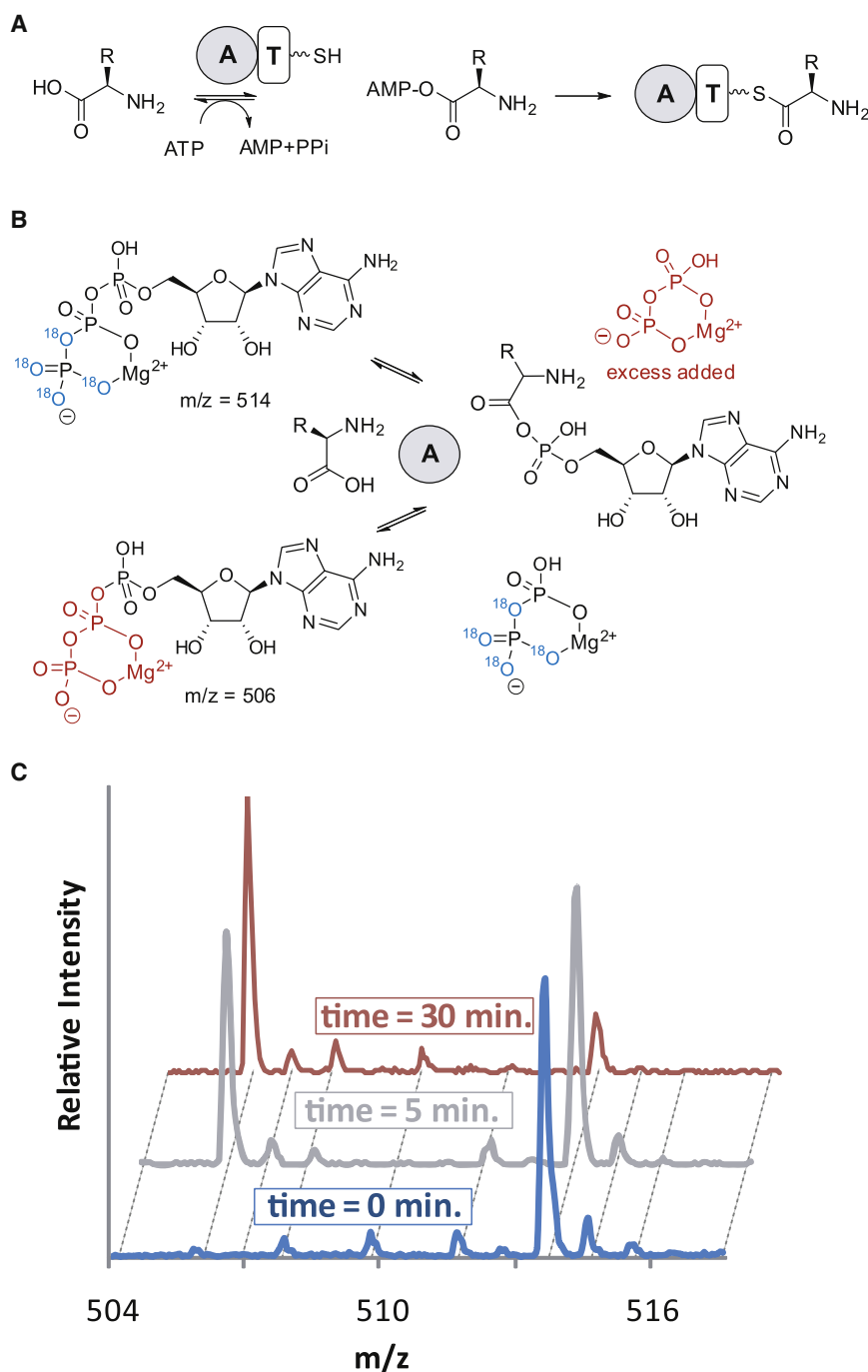


Figure 1. ATP-PP_i Exchange

(A) A domains in NRPS systems adenylate amino acids for subsequent thiolation reactions on T domains.

(B) The exchange reaction, performed in the absence of thiolation activity, measures equilibrium exchange of γ -¹⁸O₄-ATP with ¹⁶O₄-pyrophosphate.

(C) Time-dependent formation of γ -¹⁶O₄-ATP and disappearance of γ -¹⁸O₄-ATP with TycA, measured by MALDI-TOF MS. Intermediary masses correspond to ¹⁸O₃, ¹⁸O₂, and ¹⁸O₁ peaks.

ments, acetone quenched reactions were separated from salts and buffer using a graphitic matrix column (Hypercarb, Thermo Inc.), which reliably retains highly charged aromatic metabolites via charge quadrupole and hydrophobic interactions (Hu et al., 2007; Xing et al., 2004). The Hypercarb column was eluted with an isocratic gradient of 17.5% ACN/82.5% 20 mM ammonium acetate buffer and analytes were detected in negative ion mode.

Formation of γ -¹⁶O₄-ATP and consumption of γ -¹⁸O₄-ATP was directly monitored by observing the 8 Da mass shift (Figure 1C) due to back exchange of unlabeled PPI. The activity of the enzyme was quantified as the integrated peak ratio of γ -¹⁶O₄-ATP species to all ATP species in the reaction mixture. Because the species being compared are isotopologues, peak integration and the subsequent signal ratio is quantitative in both MALDI-TOF MS and ESI-LC MS because there is no difference in ionization efficiency owing to differences in chemical composition. The observed mass ratios correlate directly to the fraction of ATP-PPI exchange. Using this strategy, 5 min incubations of 6 μ l reactions can be successfully analyzed in as little as 30 s using MALDI-TOF MS. Alternatively, and with correspondingly higher sensitivity, measurements can be made with ESI-LC MS in 5 min or less.

et al., 2007) and simultaneously optimized for matrix-assisted laser desorption/ionization time-of-flight (MALDI-TOF) MS and electrospray ionization liquid chromatography (ESI-LC) MS measurement strategies. Correspondingly, adenylation domains/enzymes (200 nM) were incubated with 1 mM γ -¹⁸O₄-ATP, 1 mM amino acid, 5 mM MgCl₂, and 5 mM PPI for 5–30 min. For MALDI-TOF MS analysis, enzymatic reactions were quenched by mixing with an equal volume of 9-aminoacridine in acetone, which was found to be an optimal matrix for detection of triphosphate nucleotides (Sun et al., 2007). For ESI-LC/MS measure-

The limit of detection (LOD) for ESI-LC MS and MALDI-TOF MS was determined by mixing known amounts of labeled and unlabeled ATP in assay buffer and measuring integrated peak ratios (see Figure S2 available online). For ESI-LC MS, the LOD was determined to be 3.4 μ M (0.34% exchange), and for MALDI-TOF MS a higher LOD (10 μ M, 1% exchange) was observed. One potential source of this difference might be ion suppression effects in MALDI-TOF MS by eliminating the Hypercarb sample clean-up before analyses. Residual γ -¹⁶O₄-ATP levels found in commercial γ -¹⁸O₄-ATP were estimated to be

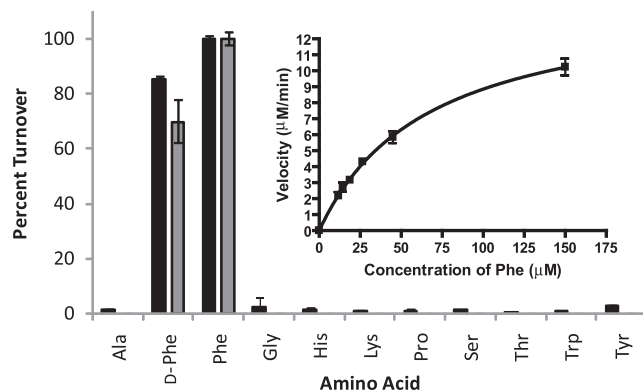


Figure 2. ESI-LC MS (■) and MALDI-TOF MS (■) Detection of TycA Substrate Activation by ATP-PPI Exchange

Inlay shows concentration dependence of exchange for L-Phe. Error bars represent standard deviations based on measurements of three reactions.

3.4 μM by ESI-LC MS and fall below the threshold of detection for the MALDI-TOF MS method. Both detection methods were comparable in sensitivity to reported radioactive ATP-PPI exchange assays. Under optimized radioactive conditions, as little as 50 pmol exchange per assay (0.01%) has been detected in a 100 μl reaction (Eigner and Lofffield, 1974). Using the rapid MALDI-TOF MS method, as little as 1% (60 pmol) exchange was detectable, whereas the full-scan ESI-LC MS method detects 0.1% (6 pmol) exchange. Further enhancement was obtained using tandem ESI-LC MS utilizing selected reaction monitoring, in which as little as 0.01% (600 fmol) exchange was detectable.

Of concern was the hydrolytic ^{18}O -lability of $\gamma\text{-}^{18}\text{O}_4\text{-ATP}$ under typical assay conditions. Correspondingly, $\gamma\text{-}^{18}\text{O}_4\text{-ATP}$ was incubated under assay conditions with (1) no TycA, (2) no amino acid, and (3) incorrect amino acid for up to 15 hr (Figure S3). Consistent with literature reports that ^{18}O -substituted phosphates are relatively stable in buffered solutions (Cohn and Hu, 1978), no loss of ^{18}O was observed at up to 15 hr in assay buffer in the absence of TycA. However, in the presence of enzyme or incorrect amino acid, slow exchange of ^{18}O label was observed after 2–5 hr. Of note, non- $\beta\text{-}\gamma$ -bridging ^{18}O atoms exchanged more rapidly than bridging ^{18}O atoms. Incubation of $\gamma\text{-}^{18}\text{O}_4\text{-ATP}$ with TycA for 5 hr resulted in a decrease in $^{18}\text{O}_4$ of 45%–60% whereas only a 14%–24% increase in the –8 Da shift, corresponding to the loss of the bridging $\beta\text{-}\gamma$ ^{18}O , was observed under the same conditions. As PPI exchange is only indicated by complete loss of bridging label, these slow shifts can be compensated for by calculating the exchange as the ratio of unlabeled ATP divided by the sum of all ATP species normalized to the theoretical equilibrium 5:1 $^{16}\text{O}/^{18}\text{O}$ molar ratio. Therefore, 83.33% apparent exchange reflects 100% exchange and % exchange = $(100/0.833) \cdot ^{16}\text{O}/(^{18}\text{O} + ^{16}\text{O})$.

TycA from tyrocidine biosynthesis has been extensively studied by the conventional ^{32}P PPI exchange assay (Lee and Lipmann, 1975; Otten et al., 2007) and was selected as a model synthetase for method development of mass-based PPI exchange. To demonstrate substrate selectivity, we tested the full panel of proteinogenic amino acids and D-phenylalanine,

Table 1. Activity of Amino Acid Adenylating Enzymes

Enzyme	Amino Acid	$\gamma\text{-}^{18}\text{O}_4\text{-ATP}$ Exchange (%)
TycA	D-Phe	69.8 ± 7.8
	L-Phe	100 ± 2.5
ORF21 ^a	HA	8.9 ± 2.3
	MHA	27.3 ± 3.2
ValA ^a	Val	5.5 ± 0.8
TrpRS ^a	Trp	9.7 ± 1.6
LysRS ^a	Lys	13.0 ± 2.7

^a Exchange measured by MALDI-TOF MS for a panel of amino acids. Exchange is only listed for active amino acids. All other amino acids tested fell below the threshold of detection for the MALDI-TOF-MS-based assay.

a previously identified substrate of TycA. As shown in Figure 2, L-phenylalanine and D-phenylalanine were both identified as substrates demonstrating 70%–100% exchange using both MALDI-TOF MS and ESI-LC MS analysis. Due to the LOD for MALDI-TOF MS, no exchange was observed for all other amino acids tested. However, the signal of MALDI-TOF MS analysis could be enhanced with increased enzyme concentration and/or longer incubation times (Figure S4). Lower rates of exchange were also effectively measured by ESI-LC MS.

To further validate the assay, an additional orphan synthetase, ValA, a valine activating A-domain identified and verified by Shen and coworkers (Du and Shen, 1999), was tested. The MALDI-TOF MS assay demonstrated appreciable levels of exchange for valine in accordance with previous studies. Again, for all other amino acids tested, levels of exchange fell below the LOD for MALDI-TOF MS analysis, but low levels of exchange were easily detectable using either ESI-LC MS analysis or longer incubation times with higher enzyme concentrations for the MALDI-TOF MS method (data not shown).

To demonstrate the applicability of the mass-based exchange assay for kinetics measurements, the exchange velocities for TycA were plotted versus phenylalanine concentration as shown in Figure 2. As previously noted, decoupled A-domains are not catalytic. Therefore, concentration-response curves of PPI exchange assays cannot be strictly interpreted in terms of Michaelis-Menten steady-state kinetics. It should be noted that a comprehensive quantitative treatment of exchange kinetics for the purposes of deriving kinetic constants has been described (Cole and Schimmel, 1970). In any event, the apparent Michaelis-Menten kinetic parameters can be calculated for the purpose of comparison to previously reported TycA apparent parameters. ESI-LC MS analysis yielded an apparent K_M of 67 ± 2 μM and apparent k_{cat} of 92 ± 2 min⁻¹. These values are consistent with previously described measurements which report measurements of K_M between 40 μM (Pfeifer et al., 1995) and 13 μM (Otten et al., 2007).

In addition to the aforementioned NRPS adenylation domains, two previously characterized tRNA synthetases from *E. coli*, TrpRS and LysRS, were also assayed using mass-based pyrophosphate exchange. As shown in Table 1, TrpRS and LysRS activate their cognate amino acids under standard assay conditions. No activation was observed for nonsubstrates (data not shown).

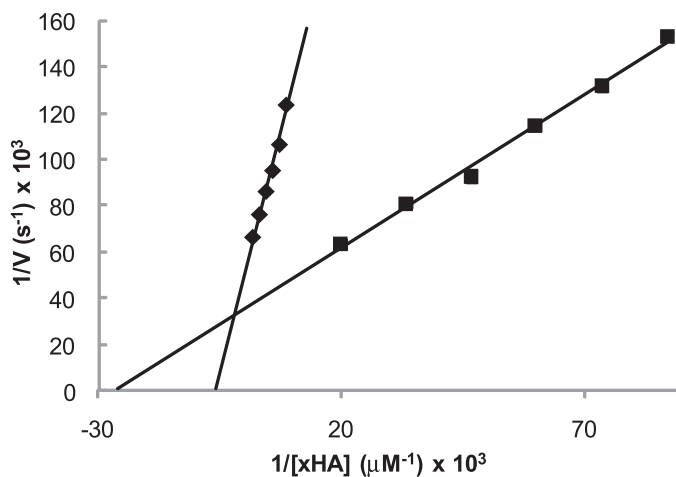
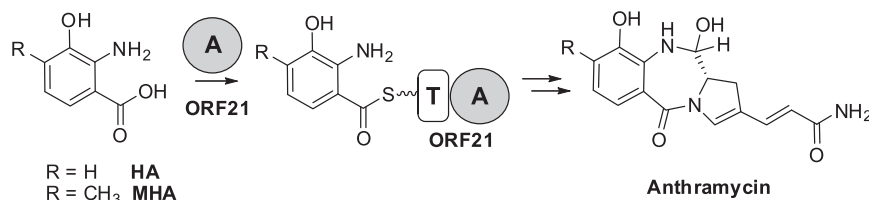


Figure 3. Exchange Kinetics of ORF21

(Above) Proposed reaction catalyzed by ORF21 en route to anthramycin. (Below) ORF21 substrate dependence of exchange for ORF21 double-reciprocal plot for MHA (■) and HA (◆), respectively. Data were measured in triplicate using the ESI-LC MS method.

DISCUSSION

New strategies are continually developed for ribosomal and nonribosomal peptide synthetase analysis and characterization (Francklyn et al., 2008; Linne and Marahiel, 2004b). For example, recently described MS methods allow the determination of aminoacyl-S-enzyme intermediates on intact proteins (Dorrestein et al., 2006; Hicks et al., 2004). Other high-throughput methods include fluorescence polarization assays, which utilize a competitive binding experiment with a synthetic fluorescent probe (Neres et al., 2008) and affinity capture techniques,

which utilize alkyne-functional probes in “click” type analysis (La Clair et al., 2004; Zou and Yin, 2008). The mass-based pyrophosphate exchange assay described herein is complementary to these methods and provides an improved alternative to the conventional ³²Pi exchange assay, an indispensable tool in synthetase investigation. Equilibrium exchange compared via mass isotopologue ratios is a direct measurement of exchange, eliminating artifacts that might result from radioisotope exchange methods. Stable isotopologues permit quantitative analyses in both MALDI-TOF MS and ESI-LC MS methods and exchange kinetics parameters can be readily determined.

Several practical advantages of the mass-based system with regard to the conventional assay are also evident. The use of stable isotopes circumvents the labor and regulatory expenses related to the safe handling of radioactive materials. In addition to γ -¹⁸O₄-ATP being indefinitely stable at -80°C , the low reaction volume used in our method (6 μl) permits over 3000 exchange reactions to be performed using 10 mg γ -¹⁸O₄-ATP, resulting in a materials cost of approximately 33 cents per reaction using commercially available starting materials. Lastly, the speed of the mass-based assay compares favorably to conventional exchange methods. ³²Pi exchange assays employ solid-phase capture, centrifugation, or thin-layer chromatography steps followed by liquid scintillation counting, typically requiring continuous monitoring of β -emission for up to 48 hr for maximal sensitivity. Conversely, mass-based detection can be performed in as little as 30 s per sample in our MALDI-TOF MS implementation, which has not yet been optimized for speed. Furthermore, the MALDI-based assay described herein requires little sample clean-up and handling prior to analysis. Future implementation with imaging MALDI-TOF MS (Cornett et al., 2007), or imaging MALDI-ion mobility-TOF MS, detection of 384-well plates could in principle accelerate the analyses to rates faster than 1 s per sample (McLean et al., 2007).

ORF21 from the thermophilic actinomycete *Streptomyces feuillius* has been proposed to encode the initiating A-T containing module of anthramycin biosynthesis (Hu et al., 2007). Previous sequence analysis and chemical complementation studies of the anthramycin pathway revealed that there are two possible substrates for ORF21 activation: 3-hydroxyanthranilic acid (HA) and 4-methyl-3-hydroxyanthranilic acid (MHA). Sequence analysis of the putative A-domain peptide sequence indicates it is highly divergent from previously studied A-domains. Analysis of residues in the substrate binding region indicate Asp-235 (GrsA numbering), essential for binding α -amino functionality, is substituted by alanine in ORF21. Furthermore, the 8 to 10 amino acid selectivity conferring code (Challis et al., 2000; Stachelhaus et al., 1999) bears no similarity to previously described A-domains including, notably, actinomycin synthase ACMS I, which has been reported to activate the MHA analog *p*-toluic acid in the MHA-containing peptide actinomycin (Pfennig et al., 1999).

To provide direct biochemical evidence for substrate activation of the A-domain of ORF21, the encoding gene was cloned via polymerase chain reaction and ligated into pETDEST-42 for overproduction as a C-terminal His₆-tagged protein and purified using Ni²⁺-affinity chromatography (Figure S1). As summarized in Table 1, purified ORF21 activates only MHA and HA, stimulating a 3-fold higher rate of exchange for MHA when the reaction mixture is incubated for 30 min at 47°C, the optimal temperature for anthramycin production. For further characterization of Orf21, apparent kinetic parameters were calculated for both MHA and HA. ESI-LC MS analysis yielded apparent K_M of $33 \pm 3 \mu\text{M}$ and apparent k_{cat} of $130 \pm 7 \text{ min}^{-1}$ for MHA and K_M of $154 \pm 9 \mu\text{M}$ and apparent k_{cat} of $99 \pm 2 \text{ min}^{-1}$ for HA (Figure 3). Although the exchange assay suggests MHA is a likely substrate for ORF21, further studies are required to pinpoint the timing of methylation during anthramycin biosynthesis.

Recently, microbial genomics initiatives have identified staggering numbers of gene clusters containing cryptic putative NRPS. Given the history of NRP drugs, these synthetases are likely to encode new natural products with potential as drug leads and bioprobes. NRPS A domain substrate selectivity can be estimated, to varying degrees of accuracy, by primary sequence analysis using homology modeling approaches or neural network algorithms (Challis et al., 2000; Rausch et al., 2005; Stachelhaus et al., 1999). However, subsequent to these *in silico* analyses, it is often necessary to provide biochemical evidence supporting A domain selectivity. The γ - $^{18}\text{O}_4$ -ATP-PPi exchange system provides a rapid, sensitive, and reproducible means to measure adenylation domain specificity. Moreover, when combined with previously reported 96-well based liquid handling methods for evaluating A-domains in *E. coli* libraries (Otten et al., 2007), it is readily adaptable to high-throughput analysis appropriate for directed evolution studies (Fischbach et al., 2007).

EXPERIMENTAL PROCEDURES

ATP-PPi Exchange Assay Conditions

In order to avoid precipitation of magnesium pyrophosphate, assay components were divided into stock solutions comprising (1) 3 mM amino acids containing 15 mM PPi in 20 mM Tris (pH 7.5), (2) 3 mM γ - $^{18}\text{O}_4$ -ATP containing 15 mM MgCl_2 in 20 mM Tris (pH 7.5), and (3) 600 nM enzyme in 20 mM Tris (pH 7.5) containing 5% glycerol and 1 mM DTT. Exchange reactions containing 2 μl of each component were initiated by the addition of enzyme solution. Therefore, 6 μl reactions contained final concentrations of 5 mM MgCl_2 , 5 mM PPi, 1 mM γ - $^{18}\text{O}_4$ -ATP, 1 mM amino acid, and 20 mM Tris-HCl (pH 7.5). After an incubation period (30 min at 25°C for TycA, ValA, TrpRS, and LysRS or 47°C for ORF21), the reactions were stopped by the addition of 6 μl 9-aminoacridine in acetone (10 mg/ml) for MALDI-TOF MS analysis or 6 μl acetone for ESI-LC MS analysis. For enhanced MALDI-TOF MS signal, 1 μM TycA was incubated for 2 hr. Detailed mass spectrometric parameters and HPLC/MS conditions are described in detail in Supplemental Data.

Data Analysis

The equilibrium molar ratio of unlabeled PPi to γ - $^{18}\text{O}_4$ -ATP under assay conditions is 5:1. Therefore, 83.33% apparent exchange corresponds to 100% exchange. Percent exchange was determined by comparison of the ratio of γ - $^{18}\text{O}_4$ -ATP to the sum of all ATP species normalized with this modifier: % exchange = $(100/0.833) \cdot \frac{^{16}\text{O}/(^{18}\text{O} + ^{16}\text{O})}{\text{sum of all ATP species}}$. Monoisotopic peak areas were determined using manufacturer's software. For MALDI-TOF MS analysis, the ratio of the area of γ - $^{18}\text{O}_4$ -ATP (m/z 506) to the area of total ATP including unlabeled, partially labeled, fully labeled, and monosodium-coordinated ions (m/z 506, 508, 510, 512, 514, 528, 530, 532, 534, 536) was calculated. For ESI-LC MS analysis, the ratio of the area of γ - $^{18}\text{O}_4$ -ATP to the area of total ATP including unlabeled, partially labeled, fully labeled, monosodium-coordinated, and sodium acetate adduct ions was similarly calculated. For selected reaction monitoring, the ratio of the area of γ - $^{18}\text{O}_4$ -ATP, taken as the area of the product ion (m/z 408), to the area of total ATP including unlabeled, partially labeled, and fully labeled ions, taken as the sum of the area of their respective product ions ([514 \rightarrow 408, 410, 412, 414, 416], [512 \rightarrow 408, 410, 412, 414], [510 \rightarrow 408, 410, 414], [508 \rightarrow 408, 410], and [506 \rightarrow 408]), was calculated.

SUPPLEMENTAL DATA

Supplemental Data include Supplemental Experimental Procedures and four figures and can be found with this article online at [http://www.cell.com/chemistry-biology/supplemental/S1074-5521\(09\)00140-9](http://www.cell.com/chemistry-biology/supplemental/S1074-5521(09)00140-9).

ACKNOWLEDGMENTS

Funding was provided by the National Institutes of Health 1R01GM077189-3 (to B.O.B.), the Vanderbilt University College of Arts and Sciences, and the

Vanderbilt Institute of Chemical Biology (to J.A.M.). We wish to acknowledge Ben Shen (University of Wisconsin) for the gift of the ValA vector, Torsten Stachelhaus (AureoGen Biosciences) for the gift of the TycA vector, Anthony Forster (Vanderbilt University) for the gift of TrpRS and LysRS, and Randi Gant-Branum and Michal Kliman for instrumental assistance (Vanderbilt University).

Received: December 29, 2008

Revised: March 27, 2009

Accepted: April 17, 2009

Published: May 28, 2009

REFERENCES

- Challis, G.L., Ravel, J., and Townsend, C.A. (2000). Predictive, structure-based model of amino acid recognition by nonribosomal peptide synthetase adenylation domains. *Chem. Biol.* 7, 211–224.
- Cohn, M., and Hu, A. (1978). Isotopic (^{18}O) shift in 31P nuclear magnetic resonance applied to a study of enzyme-catalyzed phosphate-phosphate exchange and phosphate (oxygen)-water exchange reactions. *Proc. Natl. Acad. Sci. USA* 75, 200–203.
- Cole, F.X., and Schimmel, P.R. (1970). On the rate law and mechanism of the adenosine triphosphate-pyrophosphate isotope exchange reaction of amino acyl transfer ribonucleic acid synthetases. *Biochemistry* 9, 480–489.
- Cornett, D.S., Reyzer, M.L., Chaurand, P., and Caprioli, R.M. (2007). MALDI imaging mass spectrometry: molecular snapshots of biochemical systems. *Nat. Methods* 4, 828–833.
- Dorrestein, P.C., Bumpus, S.B., Calderone, C.T., Garneau-Tsodikova, S., Aron, Z.D., Straight, P.D., Kolter, R., Walsh, C.T., and Kelleher, N.L. (2006). Facile detection of acyl and peptidyl intermediates on thioester carrier domains via phosphopantetheinyl elimination reactions during tandem mass spectrometry. *Biochemistry* 45, 12756–12766.
- Du, L., and Shen, B. (1999). Identification and characterization of a type II peptidyl carrier protein from the bleomycin producer *Streptomyces verticillus* ATCC 15003. *Chem. Biol.* 6, 507–517.
- Eigner, E.A., and Lofffield, R.B. (1974). Kinetic techniques for the investigation of amino acid: tRNA ligases (aminoacyl-tRNA synthetases, amino acid activating enzymes). *Methods Enzymol.* 29, 601–619.
- Fischbach, M.A., and Walsh, C.T. (2006). Assembly-line enzymology for polyketide and nonribosomal peptide antibiotics: Logic, machinery, and mechanisms. *Chem. Rev.* 106, 3468–3496.
- Fischbach, M.A., Lai, J.R., Roche, E.D., Walsh, C.T., and Liu, D.R. (2007). Directed evolution can rapidly improve the activity of chimeric assembly-line enzymes. *Proc. Natl. Acad. Sci. USA* 104, 11951–11956.
- Francklyn, C.S., First, E.A., Perona, J.J., and Hou, Y.M. (2008). Methods for kinetic and thermodynamic analysis of aminoacyl-tRNA synthetases. *Methods* 44, 100–118.
- Hicks, L.M., O'Connor, S.E., Mazur, M.T., Walsh, C.T., and Kelleher, N.L. (2004). Mass spectrometric interrogation of thioester-bound intermediates in the initial stages of epothilone biosynthesis. *Chem. Biol.* 11, 327–335.
- Hoard, D.E., and Ott, D.G. (1965). Conversion of mono- and oligodeoxyribonucleotides to 5-triphosphates. *J. Am. Chem. Soc.* 87, 1785–1788.
- Hu, Y., Phelan, V., Ntai, I., Farnet, C.M., Zazopoulos, E., and Bachmann, B.O. (2007). Benzodiazepine biosynthesis in *Streptomyces refuineus*. *Chem. Biol.* 14, 691–701.
- Joseph, D.R., and Muench, K.H. (1971). Tryptophanyl transfer ribonucleic acid synthetase of *Escherichia coli*. I. Purification of the enzyme and of tryptophan transfer ribonucleic acid. *J. Biol. Chem.* 246, 7602–7609.
- La Clair, J.J., Foley, T.L., Schegg, T.R., Regan, C.M., and Burkart, M.D. (2004). Manipulation of carrier proteins in antibiotic biosynthesis. *Chem. Biol.* 11, 195–201.
- Lee, S.G., and Lipmann, F. (1975). Tyrocidine synthetase system. *Methods Enzymol.* 43, 585–602.
- Linne, U., and Marahiel, M.A. (2004a). Reactions catalyzed by mature and recombinant nonribosomal peptide synthetases. *Protein Eng.* 388, 293–315.

- Linne, U., and Marahiel, M.A. (2004b). Reactions catalyzed by mature and recombinant nonribosomal peptide synthetases. *Methods Enzymol.* **388**, 293–315.
- McLean, J.A., Ridenour, W.B., and Caprioli, R.M. (2007). Profiling and imaging of tissues by imaging ion mobility-mass spectrometry. *J. Mass Spectrom.* **42**, 1099–1105.
- Neres, J., Wilson, D.J., Celia, L., Beck, B.J., and Aldrich, C.C. (2008). Aryl acid adenylating enzymes involved in siderophore biosynthesis: fluorescence polarization assay, ligand specificity, and discovery of non-nucleoside inhibitors via high-throughput screening. *Biochemistry* **47**, 11735–11749.
- Otten, L.G., Schaffer, M.L., Villiers, B.R., Stachelhaus, T., and Hollfelder, F. (2007). An optimized ATP/PP(i)-exchange assay in 96-well format for screening of adenylation domains for applications in combinatorial biosynthesis. *Bio-technol. J.* **2**, 232–240.
- Pfeifer, E., Pavela-Vrancic, M., von Dohren, H., and Kleinkauf, H. (1995). Characterization of tyrocidine synthetase 1 (TY1): requirement of posttranslational modification for peptide biosynthesis. *Biochemistry* **34**, 7450–7459.
- Pfennig, F., Schauwecker, F., and Keller, U. (1999). Molecular characterization of the genes of actinomycin synthetase I and of a 4-methyl-3-hydroxyanthranilic acid carrier protein involved in the assembly of the acylpeptide chain of actinomycin in *Streptomyces*. *J. Biol. Chem.* **274**, 12508–12516.
- Rausch, C., Weber, T., Kohlbacher, O., Wohlleben, W., and Huson, D.H. (2005). Specificity prediction of adenylation domains in nonribosomal peptide synthetases (NRPS) using transductive support vector machines (TSVMs). *Nucleic Acids Res.* **33**, 5799–5808.
- Sieber, S.A., and Marahiel, M.A. (2005). Molecular mechanisms underlying nonribosomal peptide synthesis: Approaches to new antibiotics. *Chem. Rev.* **105**, 715–738.
- Stachelhaus, T., Mootz, H.D., and Marahiel, M.A. (1999). The specificity-conferring code of adenylation domains in nonribosomal peptide synthetases. *Chem. Biol.* **6**, 493–505.
- Stern, R., DeLuca, M., Mehler, A.H., and McElroy, W.D. (1966). Role of sulfhydryl groups in activating enzymes. Properties of *Escherichia coli* lysine-transfer ribonucleic acid synthetase. *Biochemistry* **5**, 126–130.
- Sun, G., Yang, K., Zhao, Z.D., Guan, S.P., Han, X.L., and Gross, R.W. (2007). Shotgun metabolomics approach for the analysis of negatively charged water-soluble cellular metabolites from mouse heart tissue. *Anal. Chem.* **79**, 6629–6640.
- Xing, J., Apedo, A., Tymiak, A., and Zhao, N. (2004). Liquid chromatographic analysis of nucleosides and their mono-, di- and triphosphates using porous graphitic carbon stationary phase coupled with electrospray mass spectrometry. *Rapid Commun. Mass Spectrom.* **18**, 1599–1606.
- Zou, Y., and Yin, J. (2008). Alkyne-functionalized chemical probes for assaying the substrate specificities of the adenylation domains in nonribosomal peptide synthetases. *Chem. Bio. Chem.* **9**, 2804–2810.